Fish and Shellfish Immunology 91 (2019) 325–332

Contents lists available at ScienceDirect

Fish and Shellfish Immunology

journal homepage: www.elsevier.com/locate/fsi

Full length article

ATG10 (autophagy-related 10) regulates the formation of autophagosome in the anti-virus immune response of pacific oyster (*Crassostrea gigas*)

Zirong Han[a,c], Weilin Wang[a,c,*], Xiaojing Lv[a,c], Yanan Zong[a,c], Shujing Liu[a,c], Zhaoqun Liu[a,c], Lingling Wang[a,b,c,d], Linsheng Song[a,b,c,*]

[a] Liaoning Key Laboratory of Marine Animal Immunology, Dalian Ocean University, Dalian, 116023, China
[b] Functional Laboratory of Marine Fisheries Science and Food Production Processes, Qingdao National Laboratory for Marine Science and Technology, Qingdao, 266235, China
[c] Liaoning Key Laboratory of Marine Animal Immunology and Disease Control, Dalian Ocean University, Dalian, 116023, China
[d] Dalian Key Laboratory of Aquatic Animal Disease Prevention and Control, Dalian Ocean University, Dalian, 116023, China

ARTICLE INFO

Keywords:
Autophagy
ATG10
Autophagosome
Crassostrea gigas
Anti-virus immunity

ABSTRACT

Autophagy, a highly conserved intracellular degradation system, is involved in numerous processes in vertebrate and invertebrate, such as cell survival, ageing, and immune responses. However, the detailed molecular mechanism of autophagy and its immune regulatory role in bivalves are still not well understood. In the present study, an autophagy-related protein ATG10 (designated as *Cg*ATG10) was identified from Pacific oyster *Crassostrea gigas*. The open reading frame of *Cg*ATG10 cDNA was of 621 bp, encoding a polypeptide of 206 amino acid residues with an Autophagy_act_C domain (from 96 to 123 amino acid), which shared high homology with that from *C. virginica* and *Octopus bimaculoides*. The mRNA transcripts of *Cg*ATG10 were widely expressed in all the tested tissues including mantle, gonad, gills, hemocytes and hepatopancreas, with the highest expression level in mantle. After the stimulation with poly (I:C), the mRNA expression level of *Cg*ATG10 in the mantle of oysters was significantly up-regulated (4.92-fold of that in Blank group, $p < 0.05$), and the LC3-conversion from LC3-I to LC3-II (LC3-II/LC3-I) also increased. After an additional injection of dsRNA to knock-down the expression of *Cg*ATG10 (0.33-fold and 0.10-fold compared respectively with Blank group and dsGFP group, $p < 0.05$), the downstream conversion of *Cg*LC3 was inhibited significantly compared with that of the control dsGFP group, while the expression level of autophagy-initiator *Cg*Beclin1 did not change significantly. In addition, the mRNA transcripts of interferon regulatory factor *Cg*IRF-1 increased significantly in *Cg*ATG10-knockdown oysters at 12 h post poly (I:C) stimulation. All the results indicated that *Cg*ATG10 might participate in the immune response against poly (I:C) by regulating autophagosome formation and interferon system in oysters.

1. Introduction

Autophagy is an intracellular degradation pathway that is highly conserved from yeast to plants and animals [1,2]. There are various types of autophagy, including micro- and macroautophagy, as well as chaperone-mediated autophagy, and the term “autophagy” usually indicates macroautophagy unless otherwise specified [3–5]. Early in the 1950s, autophagy was first morphologically characterized in mammalian cells, but its molecular mechanism was unknown until the discovery of yeast autophagy-related (ATG) genes in 1990s [6]. So far, more than 30 ATG genes have been identified in yeast, and 15 of them (ATG1-10, 12–14, 16, 18) are conserved in mammals [7–9].

There are three main steps for vertebrate autophagy, and each step involves different ATG genes. The induction of autophagy is first triggered typically by starvation, which requires the Beclin 1 (Atg6) complex [10]. The autophagosome formation is sequentially conducted by two ubiquitin-like conjugation systems, the ATG12-ATG5 conjugate and the LC3 systems, which is the second and core step of autophagy [11]. Finally, the autophagosome is fused with lysosomes (in metazoan cells) or vacuoles (in yeast and plant cells) to degrade macromolecules with lysis ATGs (such as yeast lipase Atg15/Aut5/Cvt17) [5] into monomeric units (e.g. amino acids) for reuse. ATG10 is an important adaptor to recruit other molecules for complex conjugation and plays the key roles in the second step of autophagosome formation. Previous study has revealed that ATG10 is a new type of protein-conjugating enzyme to form the ATG12-ATG10 thioester intermediate, which then

* Corresponding authors. Liaoning Key Laboratory of Marine Animal Immunology, Dalian Ocean University, Dalian, 116023, China.
E-mail addresses: wangweilin@dlou.edu.cn (W. Wang), lshsong@dlou.edu.cn (L. Song).

https://doi.org/10.1016/j.fsi.2019.05.027
Received 22 March 2019; Received in revised form 9 May 2019; Accepted 13 May 2019
Available online 22 May 2019

Table 1
Sequences of the primers used in this study.

Primer name	Sequence (5′-3′)
oligo (dT)	GGCCACGCGTCGACTAGTACT
*Cg*ATG10-RT-F	GGACAATCGTAGACACCAAAGA
*Cg*ATG10-RT-R	TACAGAACTGGCACACCATAGC
*Cg*EF-RT-F	AGTCACCAAGGCTGCACAGAAAG
*Cg*EF-RT-R	TCCGACGTATTTCTTTGCGATGT
*Cg*ATG10-F	ATGGCGGCAGGTTCAATTTCGGA
*Cg*ATG10-R	GCTGACACAAAGTTTTCCATACTCCAGAGGA
*Cg*ATG10-EHF	CGCGATATCATGGCGGCAGGTTCAATTTCG
*Cg*ATG10-EHR	CCCAAGCTTGCTGACACAAAGTTTTCCATACTCCAG
*Cg*ATG10-Fi	GCGTAATACGACTCACTATAGGCAATGCCCACACACAAGG
*Cg*ATG10-Ri	GCGTAATACGACTCACTATAGGTTATATAACCATACACTATTTTTCAACA
GFP-Fi	GCGTAATACGACTCACTATAGGTGGTCCCAATTCTCGTGGAAC
GFP-Ri	GCGTAATACGACTCACTATAGGCTTGAAGTTGACCTTGATGCC
*Cg*LC3-RT-F	CCGATGCTTGACAAGACCAA
*Cg*LC3-RT-R	CCGTCCTCGTCTTTCTCCTG
*Cg*IRF-1-RT-F	ATTCGTGTTTTCACATTCCCTACTC
*Cg*IRF-1-RT-R	ATTTCCACCTGGTCCTCCTTATC
*Cg*Beclin-RT-F	AAATGCTGCTTGGGGTCAGA
*Cg*Beclin-RT-R	CGGAATCCACCAGACCCATA

conjugates ATG5 to form the ATG12-ATG5 conjugation [12,13]. In *Arabidopsis thaliana*, the ATG10 gene mutation induces dysfunctions of the ATG12-ATG5 conjugation and failures to accumulate autophagic bodies inside the vacuole [14]. Compared with model organisms of vertebrates and plants, the knowledge about autophagy molecular mechanisms and the detailed roles of ATGs in autophagy process is still very limited in lower invertebrates.

Recently, the immune regulation roles of autophagy are receiving increasing attentions, especially its molecular mechanisms in vertebrates [14–16]. In humans, the autophagy has been documented to function in anti-virus immunity [17,18]. Overexpression of ATG10 could facilitate the formation of autophagolysosomes and suppress the replication of HCV virus in Huh 7.5 cell line [19]. The ATG12–ATG5 conjugate was reported to suppress the type I IFN production via inhibition of retinoic acid-inducible gene I (RIG-I) and IFN-β promoter stimulator-1 (IPS-I) [20]. In Pacific oyster *Crassostrea gigas*, the anti-virus autophagy was also reported to be significantly induced by experimental infection of ostreid herpesvirus 1 (OsHV-1) [21]. However, the detailed molecular mechanism of autophagy and the roles of ATG10 in anti-virus immunity of oyster are still not well understood.

The Pacific oyster *C. gigas* is one of the important aquaculture bivalves worldwide. In the past decades, the frequent outbreak of disease has threatened the sustainable development of oyster aquaculture industry [22–25]. OsHV-1 is a virus in malacoherpesviridae family, which can infect oyster and cause mass mortality. The studies on anti-virus immunity in Pacific oyster are necessary to understand the pathological mechanism and develop the strategy to control the disease. Recently, the primitive anti-virus interferon (IFN) system containing IFN-like protein (*Cg*IFNLP) and its upstream interferon regulatory factor (*Cg*IRF-1) has been reported in *C. gigas* [26,27]. The major objectives of the present study are to (1) identify and characterize ATG10 gene in the oyster *C. gigas*, (2) clarify the involvement of *Cg*ATG10 in autophagy induced by poly (I:C), and (3) explore the modulation of ATG10 induced autophagy on the primitive interferon system in oyster antiviral immunity. The studies are helpful for further exploring the detailed molecular mechanism of autophagy and its role in anti-virus immunity in oyster.

2. Material and methods

2.1. Animals and samples collection

Pacific oysters (*C. gigas*), three years old with an average shell length of 15 cm, were collected from a local aquaculture farm (Dalian, Liaoning Province, China). The Pacific oysters were cultured in filtered and aerated seawater at 15 ± 2 °C and fed with commercial microalgae for one week prior to use. The seawater was totally replaced every day. Female mice (six-week old) were purchased from Dalian Institute of Drug Control.

Various tissues including hepatopancreas, gonad, mantle, gills and hemolymph were obtained from six oysters as parallel samples. Hemolymph was centrifuged at 800 *g*, 4 °C for 10 min to harvest the hemocytes. All the samples were stored at −80 °C in 500 μL Trizol reagent (Invitrogen) for the subsequent RNA extraction to clone cDNA and detect the distribution of *Cg*ATG10 mRNA in tissues.

2.2. RNA isolation and cDNA synthesis

Trizol reagent was used to extract the total RNA from hemocytes and other tissues according to manufacturer's instruction (Invitrogen, USA). The RNase-free DNase I (Takara, Japan) was used to digest the genomic DNA from the total RNA. Integrities of representative RNA samples were visualized via agarose gel electrophoresis assays. The quality and concentration of total RNA were estimated using a Nano Drop 2000 Spectrophotometer (Thermo Fisher Scientific, Wilmington, DE, USA). Only the RNA samples with an A260/A280 ratio between 1.8 and 2.0 were used for the subsequent analysis.

Total RNA was reverse transcribed by using the PrimeScript™ real-time PCR kit (Takara, Japan) for quantitative real-time PCR (qRT-PCR) analysis. The first-strand cDNA synthesis was performed by primer oligo (dT). One microgram of total RNA was added into the 20 μL reaction system, and the mixture was incubated at 37 °C for 15 min, and then 85 °C for 15 s. The obtained cDNA was stored at −80 °C for the subsequent qRT-PCR.

2.3. Determination of CgATG10 mRNA distribution in tissues

qRT-PCR with the primers *Cg*ATG10-RT-F and *Cg*ATG10-RT-R (Table 1) was performed to detect the distribution of *Cg*ATG10 mRNA transcripts in different tissues. A fragment of *Cg*EF (NP_001292242.2) amplified with primers *Cg*EF-RT-F and *Cg*EF-RT-R (Table 1) was used as reference. The mRNA expression levels of *Cg*ATG10 in different tissues including hepatopancreas, gonad, mantle, gill and hemocytes were determined by SYBR Green fluorescent qRT-PCR using ABI Quantstudio Sequence Detection System (Applied Biosystems). The relative expression levels of *Cg*ATG10 was analyzed by comparative Ct method ($2^{-\triangle\triangle Ct}$ method) [28].

Table 2
Sequences used for the *Cg*ATG10 alignment and phylogenetic analysis.

Gene name	Organism	Accession number
ubiquitin-like-conjugating enzyme ATG10 isoform X1	*Crassostrea gigas*	XP_011437144.1
ubiquitin-like-conjugating enzyme ATG10 isoform X2	*Crassostrea virginica*	XP_022315749.1
ubiquitin-like-conjugating enzyme ATG10	*Acanthaster planci*	XP_022100186.1
ubiquitin-like-conjugating enzyme ATG10	*Octopus bimaculoides*	XP_014777851.1
ubiquitin-like-conjugating enzyme ATG10	*Strongylocentrotus purpuratus*	XP_011664819.1
ubiquitin-like-conjugating enzyme ATG10 isoform X1	*Mizuhopecten yessoensis*	XP_021379051.1
ubiquitin-like-conjugating enzyme ATG10	*Branchiostoma belcheri*	XP_019645767.1
ubiquitin-like-conjugating enzyme ATG10 isoform X1	*Xenopus tropicalis*	XP_002935747.1
ubiquitin-like-conjugating enzyme ATG10	*Homo sapiens*	NP_001124500.1
ubiquitin-like-conjugating enzyme ATG10	*Mus musculus*	NP_080046.3
ubiquitin-like-conjugating enzyme ATG10	*Danio rerio*	NP_001032201.1

2.4. Gene cloning and sequence analysis of *CgATG10*

The primers *Cg*ATG10-F and *Cg*ATG10-R (Table 1) were designed according to the sequence information of *Cg*ATG10 (CGI_10025434) acquired from NCBI database (https://www.ncbi.nlm.gov/). The open reading frame (ORF) sequence of *Cg*ATG10 was cloned using the cDNA library of mantle. The PCR amplification was performed by using gene-specific primer *Cg*ATG10-F and *Cg*ATG10-R (Table 1) with the following protocols: 5 min at 95 °C; 30 cycles at 94 °C for 30 s, 58 °C for 45 s, 72 °C for 40 s; and 72 °C for 10 min. The PCR product was gel-purified, cloned into PMD 19-T simple vector (Takara), and confirmed by DNA sequencing.

A translation tool (http://web.expasy.org/translate/) was used to predict the amino acid sequence, theoretical molecular weight and isoelectric point of *Cg*ATG10. ClustalW Multiple Alignment program was used to conduct the multiple sequence alignment, and Simple Modular Architecture Research Tool (SMART) (http://smart.embl-heidelberg.de/) was employed to predict the conserved domain. A Neighbor-Joining (NJ) phylogenetic tree was constructed using the MEGA 5.0 [29] package with 1000 pseudo-replicates of bootstrap re-sampling to test the reliability of the branching. The numbers at the nodes indicated the bootstrap value. The scale bar corresponds to 0.05 estimated amino-acid substitutions per site.

2.5. Recombinant expression and purification of *CgATG10* protein

The ORF sequence of *Cg*ATG10 was amplified from oyster mantle by using the primers *Cg*ATG10-EHF and *Cg*ATG10-EHR (Table 1), which contained *EcoR* V and *Hind* III cleavage site sequences at the 5' end, respectively. The PCR products were gel-purified and cloned into pET-30a expression vector with a His tag. The forward positive clones were screened by PCR, and further confirmed by nucleotide sequencing. The valid recombinant plasmid was extracted and transformed into *Escherichia coli* Transetta DE3. Positive transformants were cultured in LB medium at 37 °C with shaking at 200 rpm. When the culture medium reached OD_{600} of 0.4–0.6, the bacteria were incubated for additional 8 h with the induction of Isopropyl β-D-1-Thiogalactopyranoside (IPTG) at the final concentration of 1 mM. The recombinant protein of *Cg*ATG10 (r*Cg*ATG10) with a six-His (6 × His) tag at C-terminal was purified by Ni^+ affinity chromatography, and desalted by extensive dialysis. The purified protein was concentrated and stored at −80 °C.

2.6. Preparation of polyclonal antibodies against *CgATG10*

Six-week-old mice were immunized with r*Cg*ATG10 to acquire polyclonal antibodies following the description in previous report [30]. Briefly, 100 μL r*Cg*ATG10 (0.4 mg mL^{-1}) was emulsified with 100 μL complete Freund's adjuvant (Sigma, USA) to immunize each mouse by subcutaneous implantation. The second and third injections were performed on the 14th and 21st day with incomplete Freund's adjuvant (Sigma, USA). The fourth injection was performed with 100 μL r*Cg*ATG10 on the 28th day. The anti-r*Cg*ATG10 serum was obtained on the 36th day and stored at −80 °C before use.

2.7. RNA interference assay

The cDNA fragment of *Cg*ATG10 was amplified by the primers *Cg*ATG10-Fi and *Cg*ATG10-Ri linked to the T7 promoter (Table 1), and this fragment was used as template to synthesize dsRNA of *Cg*ATG10 (ds*Cg*ATG10). dsGFP amplified with GFP-Fi and GFP-Ri (Table 1) was used as control. The dsRNA was synthesized using T7 polymerase (Takara) according to the instruction. The *in vitro* transcription system included 2 μL 10 × transcription Buffer, 2 μL (ATP + GTP + CTP + UTP solution separately), 0.5 μL RNase inhibitor, 2 μL T7 RNA polymerase and 1 μg linear template DNA, and RNase free dH_2O was added to a total of 20 μL system. The reaction was conducted at 16 °C overnight to obtain dsRNA.

After an acclimatization of seven days, thirty-six oysters were randomly divided into four groups, blank group, poly (I:C) group, dsGFP group, and ds*Cg*ATG10 group. The oysters in poly (I:C) group, dsGFP group and ds*Cg*ATG10 group were individually treated by an injection of 100 μL poly (I:C) (1 mg mL^{-1} in sterilized seawater) (Sigma, USA, synthetic stranded RNA) into the adductor muscle through the tiny hole near the shell edge, while the rest oysters in the blank group received an injection of 100 μL sterilized seawater. At 12 h after injection, the oysters of dsGFP group and ds*Cg*ATG10 group received another injection with dsGFP or ds*Cg*ATG10 (100 μL, 40 μg). To enhance the RNAi effect, a third injection with dsRNA was performed at 12 h after the second injection, and the mantle tissues were collected for mRNA and protein extraction from the oyster at 12 h after the third injection. Afterward, the total RNA was extracted and assessed by qRT-PCR with the primers *Cg*ATG10-RT-F and *Cg*ATG10-RT-R (Table 1) to evaluate the RNAi efficacy. The qRT-PCR reactions were carried out on ABI Quantstudio Sequence Detection System (Applied Biosystems) using SYBR premix ExTaq (RR420, Takara).

The relative expression levels of *Cg*ATG10, *Cg*LC3, *Cg*Beclin1 and *Cg*IRF-1 at 36 h after poly (I:C) injection were determined by qRT-PCR with specific primers (Table 1) in *Cg*ATG10-knockdown oysters. dsGFP group was used as control. Three parallel replicates were performed, and the significant and extremely differences in the unpaired sample *t*-test were accepted at $*p < 0.05$, $**p < 0.01$, respectively.

2.8. Western blot analysis of *CgATG10* and *CgLC3*

The specificity of polyclonal antibody against r*Cg*ATG10 was verified by Western blot assay. Briefly, r*Cg*ATG10 was separated by 15% SDS-PAGE, and electrophoretically transferred onto a nitrocellulose (NC) membrane. The membrane was washed three times with TBS containing 0.1% Tween 20 (TBST), blocked by 5% skimmed milk (100 mL TBST, 5 g skimmed milk) at 4 °C overnight, and then incubated with 1:1000 diluted polyclonal antibody against r*Cg*ATG10 at 37 °C for 3 h. After three times of washing with TBST, the membrane was

incubated with 1:3000 diluted secondary antibody Goat-anti-mouse IgG conjugated with HRP (ABclonal) at 37 °C for 2 h. The protein bands were developed by using Super ECL Detection Reagent (Sigma-Aldrich) for 2 min after the final three times washing with TBST, and the image was captured by Amersham Imager 600 system (GE Healthcare, USA).

The endogenous *Cg*ATG10 protein in oyster mantles was extracted from 15 to 20 mg tissue samples from each group in 1 mL of cell extraction buffer (Beyotime Biotechnology, P0013). Initially, mechanical manual grinding using pellet piston was performed and the samples were lysed in cell extraction buffer with 1 mM Phenylmethanesulfonyl fluoride (PMSF) and a protease inhibitor cocktail (Beyotime Biotechnology, ST506) on ice for 30 min. The lysates were centrifuged at 16,000 *g* 4 °C for 10 min, and the supernatant fractions were analyzed by Western blot. The first antibody was rabbit anti-LC3B (Cell Signaling Technology, LC3A/B 4108) and the secondary antibody was HRP-conjugated Goat Anti-Rabbit IgG (Sangon Biotech, D110058-0100). The remaining steps were conducted as the description above.

2.9. Statistical analysis

All the data were shown as mean ± S.D. The two-samples Student's tested was performed for the comparisons between groups. Multiple group comparisons were executed by one-way ANOVA and followed by a Tukey multiple group comparison test using Statistical Package for Social Sciences (SPSS) 16.0 Software. The difference was considered as significant at $p < 0.05$.

3. Results

3.1. The molecular features and phylogenetic relationship of CgATG10

The open reading frame of *Cg*ATG10 cDNA was of 621 bp, encoding a polypeptide of 206 amino acid residues with an isoelectric point (pI) of 5.18. The domain architectures of ATG10 proteins were predicted, and only one Autophagy_act_C domain (Fig. 1A) was identified in *Cg*ATG10. The deduced amino acid sequence of *Cg*ATG10 was aligned with that of ATG10s from other organisms, and the sequences of Autophagy_act_C domain in ATG10 protein were found to be highly conserved among different species. The conserved amino acid residues, leucine (Leu^{107}, Leu^{159}), proline (Pro^{105}, Pro^{161}), tryptophan (Trp^{125}, Trp^{141}) and the key cysteine site (Cys^{162}), were also identified in *Cg*ATG10 (Fig. 1B).

A total of ten ATG10 genes from different species were chosen to build a phylogenetic neighbor-joining (NJ) tree. All the selected ATG10 genes were distinctly divided into vertebrate and invertebrate branches. *Cg*ATG10 sharing a close evolutionary relationship with ATG10s from *C. virginica* and *Octopus bimaculoides* was clustered into the invertebrate group (Fig. 2).

3.2. Tissue distribution of CgATG10 mRNA transcripts

The distribution of *Cg*ATG10 mRNA in different tissues was investigated by quantitative real-time PCR. The mRNA transcript of *Cg*ATG10 was ubiquitously detected in all the five tested tissues, including hepatopancreas, gonad, mantle, gill and hemocytes (Fig. 3) with the highest expression level in mantle, which was approximately 2.33-fold of that in gill ($p < 0.05$).

3.3. The recombinant protein of CgATG10 and its polyclonal antibodies

The recombinant plasmid (pET-30a-*Cg*ATG10) was transfected into *E. coli* Transetta (DE3) and the recombinant expressed protein (r*Cg*ATG10) was analyzed by 15% SDS-PAGE. A distinct band of 35 kDa was observed, which was coincident with the predicted molecular weight of r*Cg*ATG10 fused with His-Tag (Fig. 4, Lane 2, Lane 3). The purified r*Cg*ATG10 was used to prepare the polyclonal antibody, and the specificity of polyclonal antibody was examined by Western blot assay. A distinct band with the similar molecular weight as r*Cg*ATG10 was revealed (Fig. 4, Lane 4), indicating the high specificity and efficiency of the polyclonal antibodies.

3.4. The expression change of CgATG10 after immune stimulation and dsRNA injection

The transcriptional level of *Cg*ATG10 in mantle was up-regulated significantly at 12 h (4.92-fold of that in Blank group, $p < 0.05$) after the stimulation with poly (I:C). But it was significantly down-regulated (0.33-fold and 0.10-fold compared respectively with Blank group and dsGFP group, Fig. 5A) by an additional injection of ds*Cg*ATG10. Meanwhile, the level of *Cg*ATG10 protein was detected by Western blot (Fig. 5B) in dsGFP group and ds*Cg*ATG10 group. The concentrations of total protein extracted from mantle tissues were normalized by using β-tubulin as a reference. There was one clear band (about 25 kDa) of *Cg*ATG10 with high specificity, which was much stranger in ds*Cg*ATG10 group than that in dsGFP group. These results manifested the successful interference of *Cg*ATG10.

3.5. The effects of CgATG10 on the formation of autophagosome

The mRNA expression level of *Cg*Beclin1 in mantle was significantly up-regulated (7.36-fold, $p < 0.05$) at 12 h after poly (I:C) injection. But there was no obvious change of *Cg*Beclin1 transcripts between the ds*Cg*ATG10 group and dsGFP group after poly (I:C) treatment in *Cg*ATG10-knockdown oysters. (Fig. 6).

Western blot analysis was employed to examine the LC3 conversion (the ratio change of LC3-I/LC3-II). Two bands, corresponding to LC3-I and LC3-II in mantle tissue, were witnessed after poly (I:C) injection compared with that of Blank group (Fig. 7). After an additional injection of ds*Cg*ATG10, the band of LC3-I became thicker compared with that in dsGFP group (Fig. 7), indicating that the LC3-II was significantly inhibited, and the ratio of LC3-I/LC3-II increased.

3.6. The expression of interferon regulatory factors (IRF) in CgATG10 knockdown oysters

In order to explore the relationship between autophagy and antivirus immune response, the relative expression of *Cg*IRF-1 mRNA was examined after autophagy was blocked. The expression level of *Cg*IRF-1 mRNA in mantle was significantly up-regulated at 12 h after poly (I:C) stimulation (8.76-fold, $p < 0.05$) compared to that in blank groups. After *Cg*ATG10 was knocked down, the expression of *Cg*IRF-1 was further up-regulated significantly (2.73-fold, $p < 0.05$) compared to that in dsGFP group (Fig. 8).

4. Discussion

Autophagy is a highly conserved subcellular degradation pathway in eukaryotes, and it plays important roles in the maintenance of cellular homeostasis as well as immune response. In the model organism *Saccharomyces cerevisiae*, more than 30 genes related to autophagy have been identified [6], among which ATG1-10, 12–14, 16–18, 29, and 31 are essential for the formation of canonical autophagosomes [31]. At present, the detailed molecular mechanism of autophagy in yeast and mammal has been well validated, which has brought great benefit to the disease treatment. However, the research on molecular component of autophagy process and its regulatory role during immune defense in bivalves is still limited.

In the present study, the evolutionarily conserved autophagy-related genes were screened from the genome of oyster *C. gigas*, and a typical ATG10 (*Cg*ATG10) gene with a conserved Autophagy_act_C domain was identified. As a core factor in the formation of autophagosomes, ATG10 has been reported to direct the final formation of

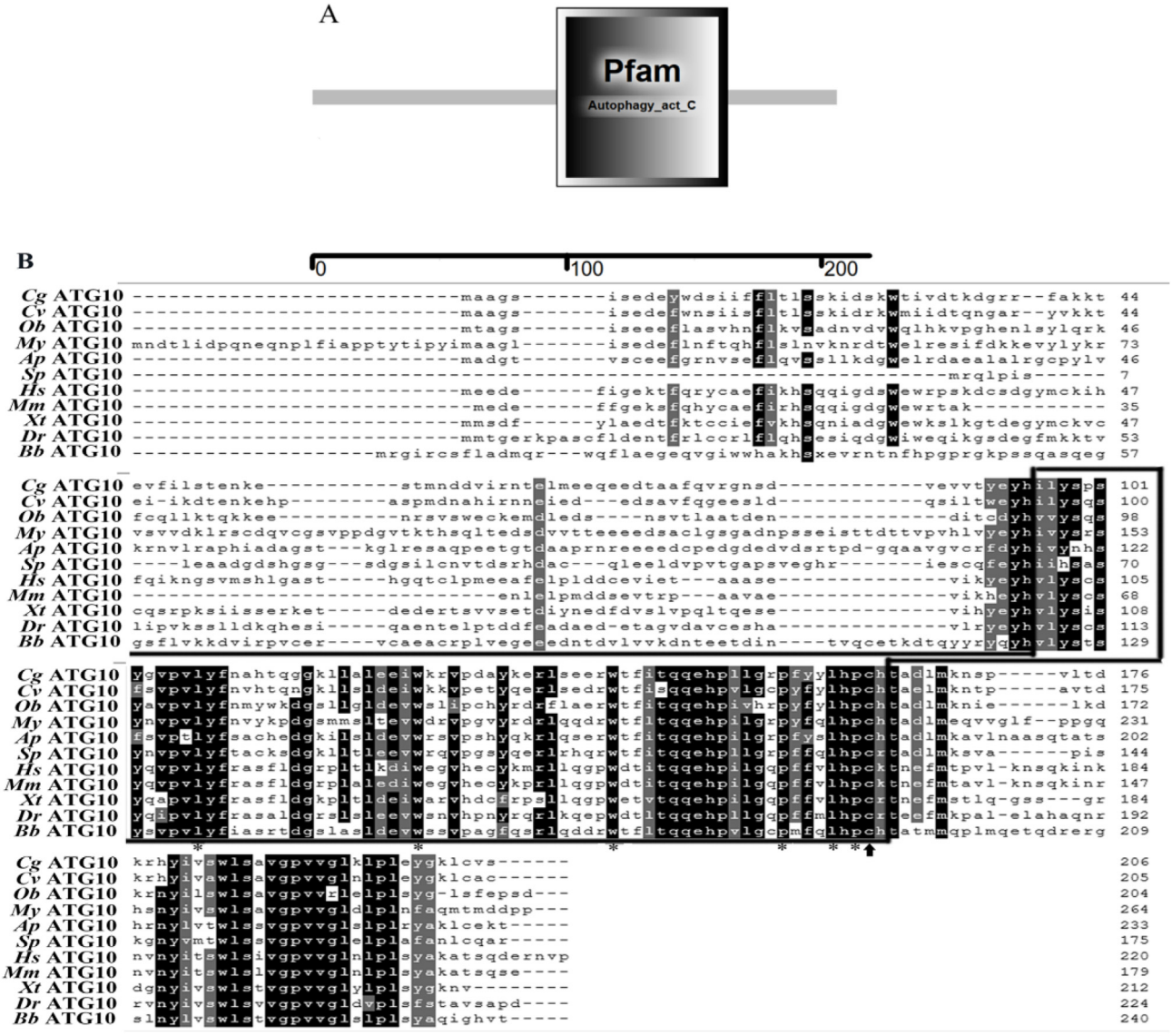

Fig. 1. Multiple sequence alignment of *Cg*ATG10 with other ATG10. (A) The structure of *Cg*ATG10 from *C. gigas* predicted by SMART. (B) Multiple sequence alignment of *Cg*ATG10 with other ATG10. Sequence information of *Ap*ATG10, *Sp*ATG10, *Cg*ATG10, *ObATG10, My*ATG10, *Hs*IRF-1ATG10, *Mm*IATG10, *Xt*ATG10, *Dr*ATG10 and *Bb*ATG10 is described in Table 2. The same amino acids are shaded in dark, similar amino acids are shaded in dark gray, and the percentage of sequence identity or similarity for coloring is 80%. The arrowhead marks the active-site cysteine (Cys 162 in *C. gigas*) involved in the forming of thioester intermediate with ATG12. Highly conserved amino acid residues among multiple Autophagy_act_C-domain containing proteins from different species are marked (*). The amino acid sequence of ATG10 domain is boxed.

ATG12-ATG5 complex in vertebrates. The only functional domain of classical ATG10 is Autophagy_act_C domain, and some key amino acid sites in this domain are thought to achieve ATG12-ATG5 conjugation in an E3-enzyme independent manner. A conserved cysteine of ATG10 can be connected to the terminal glycine of ATG12 via a thioester bond [32]. In *Cg*ATG10, the conserved amino acids, such as leucine (Leu^{107}, Leu^{159}), proline (Pro^{105}, Pro^{161}), tryptophan (Trp^{125}, Trp^{141}) and cysteine (Cys^{162}) were identified by multiple alignments, which might be the key sites for an ATG12-ATG10 thioester formation [13]. The Cys^{162} residues, highly conserved in Autophagy_act_C of all eukaryote ATG10s, was suggested to be the structural basis of thioester bond between *Cg*ATG10 and ATG12 [33]. In the phylogenetic tree, *Cg*ATG10 was firstly clustered with mollusc ATG10s from oyster *C. virginica* and octopus *O. bimaculoides* and fell in invertebrate branch. According to the high sequence homology and great similarities in molecular architecture and domain structure, *Cg*ATG10 identified from oyster *C. gigas* was confirmed to be a conserved homologue of vertebrate ATG10.

To provide a preliminary clue for the functions of *Cg*ATG10 in oysters, its expression pattern was detected by RT-PCR. The *Cg*ATG10 transcripts were ubiquitously detected in all the tested tissues. The constitutive expression of *Cg*ATG10 in various tissues suggested that autophagy was essential for multiple physiological functions, such as food digestion in hepatopancreas, gametogenesis in gonad, and immune defense in hemocytes and mantle of oyster. It has been demonstrated that autophagy plays an important role in the innate immune responses against viral, bacterial and fungal pathogens in fruit fly *Drosophila melanogaster* and nematode *Caenorhabditis elegans* [34]. In the present study, the significantly higher expression level of *Cg*ATG10 mRNA was observed in mantle. Mantle tissue of oyster is a vital immune tissue [35,36], and the external surface of mantle encounters the foreigner firstly. The immune-related genes in the mantle of oyster including recognizing molecules could be induced firstly to provide immune protective defense to provide the protective barrier in the recognition of external pathogens. Many immune related genes, such as Toll like

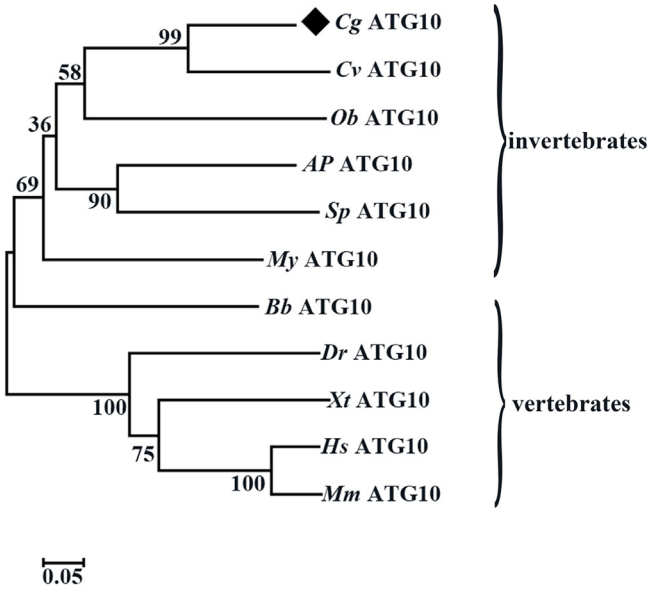

Fig. 2. Phylogenetic relationship of *Cg*ATG10 and other ten ATG10s from invertebrates and vertebrates. Sequence information is described in Table 2.

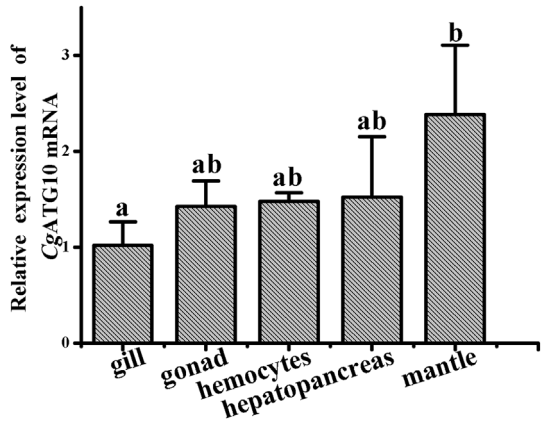

Fig. 3. The spatial expression level of *Cg*ATG10 mRNA. Relative expression levels of *Cg*ATG10 mRNA in different tissues (gill, gonad, mantle, hepatopancreas, hemocyte) were normalized to that of gill. EF was used as the internal control. Vertical bars show as mean ± S.D. (N = 6).

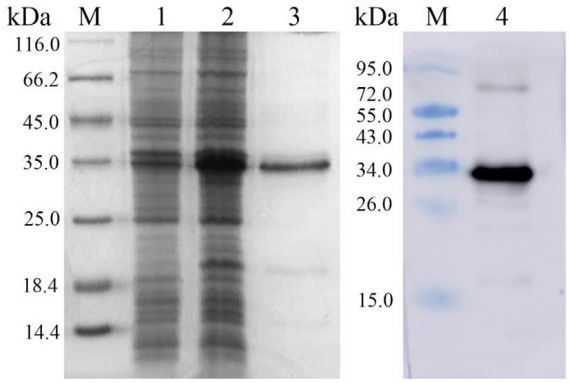

Fig. 4. SDS-PAGE and Western-blotting analysis of r*Cg*ATG10. Lane M: protein molecular standard; Lane 1: negative control for IPTG induced *E. coli* (without *Cg*ATG10); Lane 2: induced *Cg*ATG10 (the whole cell lysate); Lane 3: purified *Cg*ATG10; Lane 4: Western blot analysis of the sample in Lane 3.

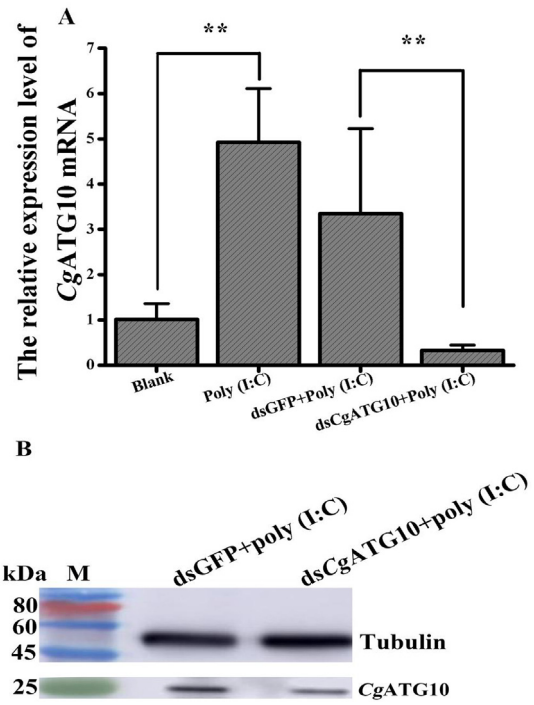

Fig. 5. Detection of interference efficiency of *Cg*ATG10. (A) The expression level of *Cg*ATG10 mRNA in mantle cells of oysters at 12 h and 36 h after poly (I:C) and ds*Cg*ATG10 injection. The dsGFP group was used as the control. Error bars represent ± S.D. of three independent repeats. Asterisks indicate significant differences (*$p < 0.05$, **$p < 0.01$). (B) The expression of *Cg*ATG10 protein in mantle tissue after ds*Cg*ATG10 injection was analyzed by western bolt.

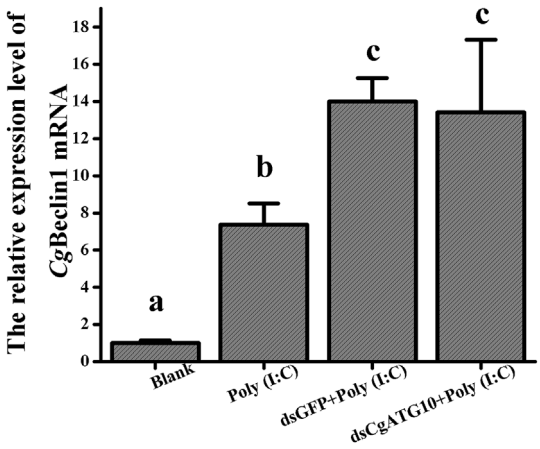

Fig. 6. The expression level of *Cg*Beclin1 mRNA in oysters after poly (I:C) injection at 36 h. The expression of *Cg*Beclin1 in mantle cells of oysters was detected by qRT-PCR at 36 h after an additional injection of dsGFP and ds*Cg*ATG10 injection. The dsGFP group was used as the control. Error bars represent ± SD of three independent repeats. Asterisks indicate significant differences ($p < 0.05$).

receptors and MDA5 (Melanoma Differentiation-Associated protein 5), are highly expressed in the mantle [37]. The high expression of *Cg*ATG10 in mantle indicated the possible immune defense role of *Cg*ATG10 in oyster. It has been reported that ATG10 participates in anti-HCV (hepatitis C virus) infection in human [19]. In the present study, the expression of *Cg*ATG10 in mantle was significantly increased after poly (I:C) injection, indicating the possible involvement of *Cg*ATG10 in response against virus stimulation. Correspondently, the upstream *Cg*Beclin1 was also significantly increased, which suggested

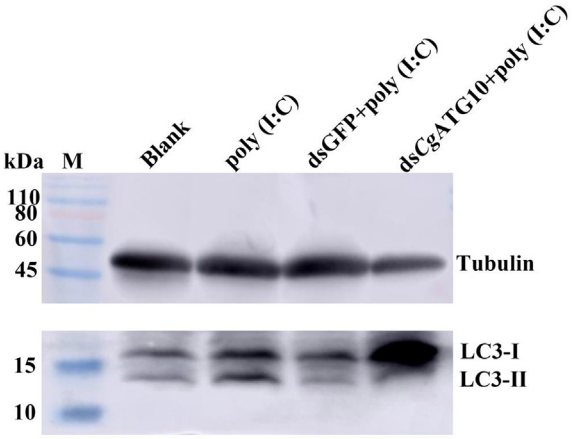

Fig. 7. Protein expression levels of LC3-I and LC3-II at 36 h after poly (I:C) stimulation. The protein expression level of LC3-I and LC3-II was tested by western blotAnd after an additional injection of dsGFP and ds*Cg*ATG10 injection.

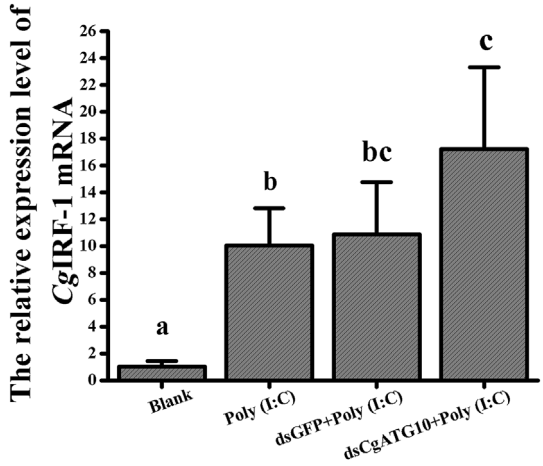

Fig. 8. The relative expression level of *Cg*IRF-1 mRNA in oysters after poly (I:C) injection. The expression level of *Cg*IRF-1 mRNA in mantle cells of oysters was detected by qRT-PCR at 36 h after an additional ds*Cg*ATG10 injection. The dsGFP group was used as the control. Error bars represent ± SD of three independent repeats. Asterisks indicate significant differences ($p < 0.05$) analyzed by *t*-test.

that an early nucleation phase stage of autophagosome formation was induced by poly (I:C) stimulation. Moreover, the autophagy biomarkers, LC3-I and LC3-II, were significantly enhanced in mantle after poly (I:C) stimulation. Therefore, it was confirmed that autophagy could be induced by poly (I:C) stimulation, and *Cg*ATG10 was involved in antivirus immune response in oysters.

The autophagy related molecules in mantle tissues were examined after the expression of *Cg*ATG10 was knocked down by dsRNA to further explore the possible role of *Cg*ATG10 in autophagy. A lower abundance of LC3-II was witnessed in ds*Cg*ATG10-injected oysters, indicating that the autophagosome formation was hindered after *Cg*ATG10 was knocked down. However, the expression of *Cg*Beclin1 did not change significantly after the injection of ds*Cg*ATG10, indicating that *Cg*ATG10 was not involved in initiation of autophagy. Beclin 1 has been reported to interact with the class III type phosphoinositide 3-kinase (PI3KC3)/Vps34 to form the Beclin 1-Vps34-Vps15 core complex, which is essential for the recruitment of other Atg proteins to the pre-autophagosomal structure (PAS) [38,39]. It has been demonstrated that Beclin 1 complex in yeast is involved in autophagosome formation at the early nucleation phase stage, rather than the following expansion step with ATG10 participation [39]. The present results suggested that the inhibition of *Cg*ATG10 could suppress the autophagy process in the oyster at the stage of autophagosome formation rather than the early nucleation phase.

The virus-induced autophagy has been reported in oyster *C. gigas* [40], but the regulatory role of autophagy in anti-virus immune response is still not clear. The IFN system is a classical anti-virus system, which has been extensively studied in vertebrates. Recently, a primitive IFN-like protein (*Cg*IFNLP) as well as an interferon regulatory factor (*Cg*IRF-1) have been identified in oyster *C. gigas,* which participate in anti-virus defense [26,27]. The link between the virus-activated autophagy process and the primitive IRF-IFN system in oyster is quit intriguing. In the present study, the expression of *Cg*IRF-1 mRNA was found to be significantly up-regulated after the oyster was treated with poly (I:C), and it was even higher expressed at 36 h after the interference of *Cg*ATG10. These results indicated that the autophagy might negatively regulate the interferon system. As the *Cg*ATG10 was induced at the late stage of immune defense, it was inferred that the enhanced autophagy might involve in inhibiting excessive response of IFN system at the recovery period of immune response. The accumulating evidences have revealed that this intracellular degradation system of autophagy plays an important role in regulation of inflammatory responses [41]. All these results indicate that the ATG10 in oyster could inhibit the expression of *Cg*IRF-1 and might negatively regulate the function of the interferon system during the anti-virus immune response.

In conclusion, an ATG10 homolog (*Cg*ATG10) with a conserved globular Autophagy_act_C domain was identified from Pacific oyster *C. gigas*. *Cg*ATG10 was constitutively expressed in all the tested tissues and highly expressed in immune-related tissue of mantle. The mRNA expression of *Cg*ATG10 in mantle was significantly up-regulated after poly (I:C) stimulation. *Cg*ATG10 might be involved in oyster innate immune response by regulating the autophagosome formation of autophagy, which could inhibit the expression of *Cg*IRF-1 and negatively regulate the interferon system during anti-virus immune response. These results would provide referential information about the autophagy process in bivalves, and also be valuable for better understanding the anti-viral mechanisms in invertebrates.

Acknowledgements

We are grateful to all the laboratory members for their technical advice and helpful discussions. This research was supported by National Key R&D Projects (2018YFD0900502), a grant from National Science Foundation of China (No. U1706204), earmarked funds from Modern Agro-industry Technology Research System (CARS-49), and the Fund for Outstanding Talents and Innovative Team of Agricultural Scientific Research, the Distinguished Professor of Liaoning (to L. S.), Key R&D Program of Liaoning Province (201703148 to L. W.), and Natural Science Foundation of Liaoning, China (20170520056), AoShan Talents Cultivation Program Supported by Qingdao National Laboratory for Marine Science and Technology (No. 2017ASTCP-OS13), Dalian High Level Talent Innovation Support Program (2015R020), and Talented Scholars in Dalian Ocean University (to L. W).

References

[1] D.J. Klionsky, K. Abdelmohsen, A. Abe, M.J. Abedin, H. Abeliovich, A. Acevedo Arozena, et al., Guidelines for the use and interpretation of assays for monitoring autophagy, Autophagy 12 (1) (2016) 1–222.
[2] B. Ravikumar, S. Sarkar, J.E. Davies, M. Futter, M. Garcia-Arencibia, Z.W. Green-Thompson, et al., Regulation of mammalian autophagy in physiology and pathophysiology, Physiol. Rev. 90 (4) (2010) 1383–1435.
[3] D.J. Klionsky, The molecular machinery of autophagy: unanswered questions, J. Cell Sci. 118 (Pt 1) (2005) 7.
[4] A.C. Massey, C. Zhang, A.M. Cuervo, Chaperone-mediated autophagy in aging and disease, Curr. Top. Dev. Biol. 73 (2006) 205–235.
[5] N. Mizushima, Autophagy: process and function, Genes Dev. 21 (22) (2007) 2861.

[6] D.J. Klionsky, Autophagy revisited: a conversation with Christian de Duve, Autophagy 4 (6) (2008) 740–743.
[7] D.J. Klionsky, E.H. Baehrecke, J.H. Brumell, C.T. Chu, P. Codogno, A.M. Cuervo, et al., A comprehensive glossary of autophagy-related molecules and processes, Autophagy 6 (4) (2010) 438–448 2nd edition.
[8] T.X. Jordan, G. Randall, Manipulation or capitulation: virus interactions with autophagy, Microb. Infect. 14 (2) (2012) 126–139.
[9] D.J. Klionsky, J.M. Cregg, W.A.D. Jr, S.D. Emr, Y. Sakai, I.V. Sandoval, et al., A unified nomenclature for yeast autophagy-related genes, Dev. Cell 5 (4) (2003) 539–545.
[10] P. Sophie, E. Lucile, B.P. Martine, C. Patrice, Regulation of macroautophagy by mTOR and Beclin 1 complexes, Biochimie 90 (2) (2008) 313–323.
[11] H. Abeliovich, W.A.D. Jr, J. Kim, D.J. Klionsky, Dissection of autophagosome biogenesis into distinct nucleation and expansion steps, J. Cell Biol. 151 (5) (2000) 1025–1033.
[12] A.R. Phillips, A. Suttangkakul, R.D. Vierstra, The ATG12-conjugating enzyme ATG10 is essential for autophagic vesicle formation in *Arabidopsis thaliana*, Genetics 178 (3) (2008) 1339–1353.
[13] T. Shintani, N. Mizushima, Y. Ogawa, A. Matsuura, T. Noda, Y. Ohsumi, Apg10p, a novel protein-conjugating enzyme essential for autophagy in yeast, EMBO J. 18 (19) (1999) 5234–5241.
[14] K. Xie, C. Liang, Q. Li, C. Yan, C. Wang, Y. Gu, et al., Role of ATG10 expression quantitative trait loci in non-small cell lung cancer survival, Int. J. Cancer 139 (7) (2016) 1564–1573.
[15] J. Ohshima, Y. Lee, M. Sasai, T. Saitoh, M.J. Su, N. Kamiyama, et al., Role of mouse and human autophagy proteins in IFN-γ-induced cell-autonomous responses against Toxoplasma gondii, J. Immunol. 192 (7) (2014) 3328.
[16] S.T. Shibutani, T. Saitoh, H. Nowag, C. Münz, T. Yoshimori, Autophagy and autophagy-related proteins in the immune system, Nat. Immunol. 16 (10) (2015) 1014.
[17] L.J. Martin, J. Gupta, S.S. Jyothula, M.B. Kovacic, J.M.B. Myers, T.L. Patterson, et al., Functional variant in the autophagy-related 5 gene promotor is associated with childhood asthma, PLoS One 7 (4) (2012) e33454.
[18] Y. Li, H. Zhu, X. Zeng, J. Fan, X. Qian, S. Wang, et al., Suppression of autophagy enhanced growth inhibition and apoptosis of interferon-β in human glioma cells, Mol. Neurobiol. 47 (3) (2013) 1000–1010.
[19] Q. Zhao, Z.Y. Hu, J.P. Zhang, J.D. Jiang, Y. Ma, J. Li, et al., Dual roles of two isoforms of autophagy-related gene ATG10 in HCV-subgenomic replicon mediated autophagy flux and innate immunity, Sci. Rep. 7 (1) (2017) 11250.
[20] S. Shoji-Kawata, B. Levine, Autophagy, antiviral immunity, and viral countermeasures, Biochim. Biophys. Acta 1793 (9) (2009) 1478–1484.
[21] P. Moreau, K. Moreau, A. Segarra, D. Tourbiez, M.A. Travers, D.C. Rubinsztein, et al., Autophagy plays an important role in protecting Pacific oysters from OsHV-1 and *Vibrio aestuarianus* infections, Autophagy 11 (3) (2015) 516–526.
[22] C. Jenkins, P. Hick, M. Gabor, Z. Spiers, S.A. Fell, X. Gu, et al., Identification and characterisation of an ostreid herpesvirus-1 microvariant (OsHV-1 μ-var) in *Crassostrea gigas* (Pacific oysters) in Australia, Dis. Aquat. Org. 105 (2) (2013) 109–126.
[23] S.E. Keeling, C.L. Brosnahan, R. Williams, E. Gias, M. Hannah, R. Bueno, et al., New Zealand juvenile oyster mortality associated with ostreid herpesvirus 1-an opportunistic longitudinal study, Dis. Aquat. Org. 109 (3) (2014) 231–239.
[24] D.R. Le, T. Renault, Purification and partial genome characterization of a herpes-like virus infecting the Japanese oyster, *Crassostrea gigas*, J. Gen. Virol. 80 (5) (1999) 1317–1322 Pt 5.
[25] A. Segarra, J.F. Pépin, I. Arzul, B. Morga, N. Faury, T. Renault, Detection and description of a particular Ostreid herpesvirus 1 genotype associated with massive mortality outbreaks of Pacific oysters, *Crassostrea gigas* , in France in 2008, Virus Res. 153 (1) (2010) 92–99.
[26] R. Zhang, R. Liu, W. Wang, L. Xin, L. Wang, C. Li, et al., Identification and functional analysis of a novel IFN-like protein (CgIFNLP) in *Crassostrea gigas*, Fish Shellfish Immunol. 44 (2) (2015) 547–554.
[27] M. Lu, C. Yang, M. Li, Q. Yi, G. Lu, Y. Wu, et al., A conserved interferon regulation factor 1 (IRF-1) from Pacific oyster *Crassostrea gigas* functioned as an activator of IFN pathway, Fish Shellfish Immunol. 76 (2018) 68–77.
[28] S. Yu, H. Liu, L. Luo, Analysis of Relative Gene Expression Using Different Real-Time Quantitative PCR, (2007).
[29] K. Tamura, D. Peterson, N. Peterson, G. Stecher, M. Nei, S. Kumar, MEGA5: molecular evolutionary genetics analysis using maximum likelihood, evolutionary distance, and maximum parsimony methods, Mol. Biol. Evol. 28 (10) (2011) 2731.
[30] S. Cheng, W. Zhan, J. Xing, X. Sheng, Development and characterization of monoclonal antibody to the lymphocystis disease virus of Japanese flounder *Paralichthys olivaceus* isolated from China, J. Virol Methods 135 (2) (2006) 173–180.
[31] N. Mizushima, T. Yoshimori, Y. Ohsumi, The role of Atg proteins in autophagosome formation, Annu. Rev. Cell Dev. Biol. 27 (1) (2011) 107–132.
[32] Y. Ohsumi, Molecular dissection of autophagy: two ubiquitin-like systems, Nat. Rev. Mol. Cell Biol. 2 (3) (2001) 211–216.
[33] S.E. Kaiser, Y. Qiu, J.E. Coats, K. Mao, D.J. Klionsky, B.A. Schulman, Structures of Atg7-Atg3 and Atg7-Atg10 reveal noncanonical mechanisms of E2 recruitment by the autophagy E1, Autophagy 9 (5) (2013) 778–780.
[34] C.-J. Kuo, M. Hansen, E. Troemel, Autophagy and innate immunity: insights from invertebrate model organisms, Autophagy 14 (2) (2018) 233–242.
[35] P. Schmitt, J.D. Lorgeril, Y. Gueguen, E. Bachère, Expression, tissue localization and synergy of antimicrobial peptides and proteins in the immune response of the oyster *Crassostrea gigas*, Dev. Comp. Immunol. 37 (3–4) (2012) 363–370.
[36] J.S. Ballantyne, J.A. Berges, Enzyme activities of gill, hepatopancreas, mantle, and adductor muscle of the oyster (*Crassostrea virginica*) after changes in diet and salinity, Can. J. Fish. Aquat. Sci. 48 (6) (1991) 1117–1123.
[37] T.J. Green, K. Benkendorff, N. Robinson, D. Raftos, P. Speck, Anti-viral gene induction is absent upon secondary challenge with double-stranded RNA in the Pacific oyster, *Crassostrea gigas*, Fish Shellfish Immunol. 39 (2) (2014) 492–497.
[38] K. Suzuki, Y. Ohsumi, Molecular machinery of autophagosome formation in yeast, *Saccharomyces cerevisiae*, FEBS Lett. 581 (11) (2007) 2156–2161.
[39] R. Kang, H.J. Zeh, M.T. Lotze, D. Tang, The Beclin 1 network regulates autophagy and apoptosis, Cell Death Differ. 18 (4) (2011) 571.
[40] M. Pierrick, M. Kevin, S. Amélie, T. Delphine, T. Marie-Agnès, D.C. Rubinsztein, et al., Autophagy plays an important role in protecting Pacific oysters from OsHV-1 and Vibrio aestuarianus infections, Autophagy 11 (3) (2015) 516–526.
[41] V. Deretic, T. Saitoh, S. Akira, Autophagy in infection, inflammation and immunity, Nat. Rev. Immunol. 13 (10) (2013) 722–737.